Heliyon 10 (2024) e31727

Contents lists available at ScienceDirect

Heliyon

journal homepage: www.cell.com/heliyon

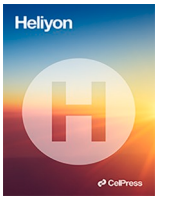

Research article

Soluble form of the MDA5 protein in human sera

Masaki Okamoto [a], Yoshiaki Zaizen [a], Shinjiro Kaieda [a], Takashi Nouno [a], Takuma Koga [a], Goushi Matama [a], Masahiro Mitsuoka [b], Jun Akiba [c], Shintaro Yamada [d], Hiroki Kato [d], Tomoaki Hoshino [a,e,*]

[a] *Division of Respirology, Neurology, and Rheumatology, Department of Medicine, Kurume University School of Medicine, 67 Asahi-machi, Kurume, Fukuoka, 830-0011, Japan*
[b] *Department of Surgery, Kurume University School of Medicine, 67 Asahi-machi, Kurume, Fukuoka, 830-0011, Japan*
[c] *Department of Pathology, Kurume University School of Medicine, 67 Asahi-machi, Kurume, Fukuoka, 830-0011, Japan*
[d] *Institute of Cardiovascular Immunology, University Hospital Bonn, University of Bonn, Venusberg-Campus 1, 53127, Bonn, Germany*
[e] *National Cancer Institute (NCI) – Frederick, 1050 Boyles St, Frederick, MD, 21702, USA*

ARTICLE INFO

Keywords:
MDA5
RNA virus
Soluble form
RNA sensor

ABSTRACT

Viral double-stranded RNA (dsRNA) is sensed by toll-like receptor 3 (TLR3) and retinoic acid-inducible gene I (RIG-I)-like receptors (RLRs), including melanoma differentiation-associated gene 5 (MDA5). MDA5 recognizes the genome of dsRNA viruses and replication intermediates of single-stranded RNA viruses. MDA5 also plays an important role in the development of autoimmune diseases, such as Aicardi-Goutieres syndrome and type I diabetes. Patients with dermatomyositis with serum MDA5 autoantibodies (anti-CADM-140) are known to have a high risk of developing rapidly progressive interstitial lung disease and poor prognosis. However, there have been no reports on the soluble form of MDA5 in human serum. In the present study, we generated in-house monoclonal antibodies (mAbs) against human MDA5. We then performed immunohistochemical analysis and sensitive sandwich immunoassays to detect the MDA5 protein using two different mAbs (clones H27 and H46). As per the immunohistochemical analysis, the MDA5 protein was moderately expressed in the alveolar epithelia of normal lungs and was strongly expressed in the cytoplasm of lymphoid cells in the tonsils and acinar cells of the pancreas. Interestingly, soluble MDA5 protein was detectable in the serum, but not in the urine, of healthy donors. Soluble MDA5 protein was also detectable in the serum of patients with dermatomyositis. Immunoblot analysis showed that human cells expressed a 120 kDa MDA5 protein, while the 60 kDa MDA5 protein increased in the supernatant of peripheral mononuclear cells within 15 min after MDA5 agonist/double-strand RNA stimulation. Hydrogen deuterium exchange mass spectrometry revealed that an anti-MDA5 mAb (clone H46) bound to the epitope (415QILENSLLNL424) derived from the helicase domain of MDA5. These results indicate that a soluble MDA5 protein containing the helicase domain of MDA5 could be rapidly released from the cytoplasm of tissues after RNA stimulation.

* Corresponding author. Division of Respirology, Neurology, and Rheumatology, Department of Medicine, Kurume University School of Medicine, 67 Asahimachi, Kurume, Fukuoka, 830-0011, Japan.
E-mail address: hoshino@med.kurume-u.ac.jp (T. Hoshino).

https://doi.org/10.1016/j.heliyon.2024.e31727
Received 15 October 2022; Received in revised form 20 May 2024; Accepted 21 May 2024
Available online 24 May 2024

1. Introduction

Abbreviations

RNAs	ribonucleic acids
DNA	deoxyribonucleic acid
ssRNA	single-stranded RNA
dsRNA	double strand RNA
RIG-I	retinoic acid-inducible gene I
RLRs	RIG-I-like receptors
MDA5	melanoma differentiation-associated gene 5
mAbs	monoclonal antibodies
CARD	caspase recruitment domains
IRF	interferon-regulatory factor
PBS	phosphate-buffered saline
AGS	Aicardi-Goutieres syndrome
DM	dermatomyositis
CADM	clinically amyopathic dermatomyositis
TLRs	toll-like receptors

Viral double-stranded RNA (dsRNA) is sensed by toll-like receptor 3 (TLR3), RIG-I-like receptors (RLRs), a family comprising RIG-I (DDX58), laboratory of genetics and physiology 2 (LGP2; DHX58), and melanoma differentiation-associated gene 5 (MDA5; IFIH1). All three RLRs are expressed in the cytoplasm (reviewed in Ref. [1]). MDA5 is activated upon infection with picornaviruses, including polio-and encephalomyocarditis viruses, as well as by long double-stranded RNA (dsRNA) [2]. MDA5 can also recognize single-stranded RNA (ssRNA) viruses of the murine coronavirus, mouse hepatitis virus, calicivirus, flavivirus families, and SARS-CoV-2 [3,4]. RIG-I and MDA5 contain two caspase recruitment domains (CARD) a DExD/H-box helicase domain composed of helicase domains 1 (Hel1) and 2 (Hel2), and a helicase insertion domain (Hel2i) [1]. MDA5 recognizes viral RNA and activates NF-κB and interferon-regulatory factor (IRF) through mitochondrial antiviral signaling, also known as IPS-1/VISA/Cardif, leading to the production of cytokines including type I and III interferons (IFNs) [5]. A previous study reported the case of a patient with a homozygous missense mutation in the Hel1 domain of MDA5 (K365E). This patient had a history of life-threatening recurrent respiratory tract infections caused by ssRNA viruses (including human rhinovirus, influenza virus, respiratory syncytial virus, and coronavirus), adenovirus, and bacteria, such as *Haemophilus influenza, Mycoplasma pneumoniae,* and *Staphylococcus aureus* [6]. Taken together, these observations indicate that MDA5 plays an important role in defense against dsRNA viruses, ssRNA viruses, deoxyribonucleic acid (DNA) viruses, and bacteria.

MDA5 is also associated with autoimmune diseases. A gain-of-function mutation in mouse MDA5 (G821S) following exposure to N-ethyl-N-nitrosourea (ENU) induces autoimmune disorders observed in interferonopathy patients, including Aicardi-Goutieres syndrome (AGS)-like encephalitis and lupus-like nephritis [7,8]. A genome-wide association study showed that single nucleotide polymorphisms (SNPs) in IFIH1 (E627* and I923V), which are loss-of-function mutations [9], are significantly associated with resistance to type 1 diabetes mellitus [10]. Six gain-of-function mutations (rare SNPs) in MDA5 have been identified in AGS in patients [11,12]. These results suggested that MDA5 plays an important role in the development of autoimmune diseases.

Dermatomyositis (DM) is an autoimmune disease characterized by the shared features of proximal skeletal muscle weakness and inflammation. Some patients with DM have definite cutaneous manifestations of DM but no clinically significant myopathy, which is defined as clinically amyopathic dermatomyositis (CADM) [13]. An anti-CADM 140 antibody has been reported to be highly expressed in patients with CADM. Patients with CADM have a high risk of developing rapidly progressive interstitial lung disease (ILD) and poor prognosis due to poor therapeutic response [14]. In 2005, an anti-CADM 140 antibody present in the sera of patients with CADM was reported to react with human MDA5 protein [15]. We previously reported anti-MDA5 antibodies as biomarkers of DM-ILD and demonstrated that the presence and titer of anti-MDA5 antibodies are associated with mortality in the early phase and/or response to immunosuppressive therapy [16,17]. A recent meta-analysis showed that anti-MDA5 antibodies could be used as biomarkers for the clinical diagnosis of DM and that the presence of anti-MDA5 antibodies is associated with poor survival [18].

As mentioned previously, MDA5 expression is highly correlated with various systemic diseases. Toll-like receptors (TLRs), which are related to innate immunity, such as MDA5, the presence of soluble forms has been reported for TLR2 and TLR4 [19,20]. We hypothesized that a soluble form of MDA5 and the presence of soluble MDA5 may influence many systemic diseases.

In the present study, we developed five in-house monoclonal antibodies against human MDA5. We performed immunohistochemical analysis and developed a sensitive sandwich immunoassay system to detect soluble MDA5 protein in sera. Soluble MDA5 protein was detected in the sera of 14 of the 32 healthy donors. Soluble MDA5 protein was also detected in the sera of 26 of 31 patients with DM. In addition, levels of the 60 kDa MDA5 protein increased in the supernatant of peripheral mononuclear cells within 15 min of dsRNA stimulation. Our *in vitro* study suggests that soluble MDA5 is rapidly released from the cytoplasm of tissues after RNA stimulation. The possible physiological role of the soluble MDA5 protein in viral infections and autoimmune diseases is also discussed.

2. Materials and methods

2.1. Human participants

Normal lung tissues were obtained from two patients with squamous carcinoma of the lung who underwent lobectomy at the Kurume University Hospital. Donor 1 was a 67-year-old male and donor 2 was a 71-year-old male. Serum and/or urine samples were obtained from 32 healthy donors (23 males and 9 females, aged 28–58 years). Formalin-fixed, paraffin-embedded tissues of the tonsils (4-year-old female) and pancreas (51-year-old female) were purchased from Bio-Options, Inc. (Brea, CA, USA). The present study also included 31 patients diagnosed with DM (9 males and 22 females, aged 12–87 years) at our institution between 2014 and 2019. The patients met the diagnostic criteria for polymyositis and dermatomyositis, as reported by Bohan and Peter [21] and recently by us [22]. Twelve of 31 patients showed seropositive for anti-MDA5 antibodies.

2.2. Recombinant full-length human MDA5 protein

Recombinant full-length human MDA5 protein was made as previously reported [23].

2.3. Establishment of an anti-human MDA5 monoclonal antibody (mAb)

Mouse anti-human MDA5 mAbs were established, and purified anti-human MDA5 mAb was generated as described previously [23, 24].

2.4. Immunoprecipitation and western blotting analysis

HEK293T cells were transfected with pEF-Flag-human MDA5 or pEF-Flag-mouse MDA5 using the pEF-BOS-EX vector [25] as previously reported [26]. At 18–48 h post-transfection, the cells were harvested and lysed with Nonidet P-40 (NP-40) lysis buffer (50 mM Tris-HCl pH 8.0, 150 mM NaCl, and 1 % NP-40) supplemented with 1 mM phenylmethylsulfonyl fluoride (PMSF), 1 mM sodium orthovanadate, and 2 μg/mL leupeptin. Subsequently, 500 μL of lysates were incubated with 1 μg of monoclonal anti-MDA5 antibodies and anti-Flag M2 (catalog no.: F3165, Sigma-Aldrich, Germany) or normal mouse IgG (catalog no.: sc-2025, Santa Cruz Biotechnology, Germany) for 30 min on ice, followed by further incubation with Dynabeads Protein G (catalog no.: 10-003-D, Invitrogen, Germany) at 4 °C overnight. The beads were eluted with 1 × SDS sample buffer (62.5 mM Tris-HCl pH 6.8, 5 % 2-mercaptoethanol, 2 % SDS, 10 % glycerol, and 0.005 % bromophenol blue) and heated for 5 min at 95 °C. Diluted (1 %) lysates of Flag-human MDA5 overexpressing HEK293T cells or Flag-mouse MDA5 overexpressing HEK293T cells were used as positive controls. The eluted proteins were analyzed using western blotting. Western blotting was performed using NuPAGE® 4–20 % Tris-Glycine Mini Gels or 7 % Tris-Acetate Midi Gel (Thermo Fisher Scientific, Tokyo, Japan) according to the manufacturer's protocol. In this study, an anti-human MDA5 mAb clone H27 and anti-β-action mAb (clone AC-15, Sigma, Tokyo, Japan) were used for western blotting.

2.5. Real-time quantitative-PCR (RT-qPCR)

cDNAs isolated from normal human tissues (lungs, spleen, pancreas, muscle, and placenta) were purchased from BioChain (Newark, CA, USA). RT-qPCR was performed twice with SYBR Green Mastermix (Qiagen, Tokyo, Japan) using primers for human β-actin and MDA5 (Qiagen) on an Mx3000p PCR machine (Stratagene, La Jolla, CA). Relative mRNA expression of MDA5 per β-actin was calculated using the comparative threshold cycle (Ct) method, using the delta delta Ct (ΔΔCt) method. Fold gene expression = 2^-(ΔΔCt), as previously reported [27,28].

2.6. Immunohistochemical staining

Immunohistochemical staining was performed using as reported [24,29]. We used an in-house mouse anti-human MDA5 mAb (H27 [mouse IgG1], 1–2 μg/mL). Mouse IgG1 (BioLegend, Tokyo, Japan) was used as control.

2.7. PBMC isolation and in vitro stimulation by polyinosinic-polycytidylic acid sodium salt (poly I:C)

Peripheral blood mononuclear cells (PBMCs) were isolated from the peripheral blood of three healthy donors using Lymphoprep™ (STEMCELL TECHNOLOGIES, Vancouver, Canada). The cells were washed twice with cold phosphate-buffered saline (PBS) and suspended in cold PBS or RPMI-1640 (Sigma) at a density of 2×10^6 cells/mL. Cells were stimulated with 250 μg/mL poly I:C (catalog no.: P1530, Merk, Tokyo, Japan) at 37 °C. Supernatants and cells were harvested at various time points.

2.8. Establishing human MDA5 sandwich immunoassay system

The human MDA5 sandwich immunoassay system was established using electrochemiluminescence in a MESOSCALE DISCOVERY ® assay system (Meso Scale Japan, Tokyo, Japan). Briefly, mouse anti-human MDA5 mAb (clone H46) was used as the primary mAb, dissolved at 2 μg/mL in PBS, dispensed into plates in aliquots of 25 μL/well, and left undisturbed overnight at 4 °C. The plates were

then washed three times with 150 μL Quantikine Wash Buffer 1 (R&D Systems, Minneapolis, MN, USA). Block Ace blocking solution (100 μL/well; Nacalai Tesque, Kyoto, Japan) was added and incubated for at least 1 h at 20 °C to prevent nonspecific adhesion of the secondary antibody to the plates. The plates were then washed three times. The samples were aliquoted at 25 μL/well. Recombinant human MDA5 protein diluted to 50, 10, 2, 400, 80, 16, and 3.2 pg/mL was used as the standard. After incubation for 1 h at 20 °C, each well was washed three times. Next, 2 μg/mL biotin-labeled mouse anti-human MDA5 secondary mAb (clone H27) was added at 25 μL/well, followed by incubation for 1 h at 20 °C after which each well was washed three times. This was followed by the addition of 50 μL of 0.5 μg/mL MSD SULFO-TAG™ labeled streptavidin to each well, and the plates were left for 30 min at 20 °C. Each well was washed three times. The amount of human MDA5 protein was measured using a MESO QuickPlex SQ 120, according to the manufacturer's protocol.

2.9. Hydrogen deuterium exchange mass spectrometry

Hydrogen deuterium exchange mass spectrometry experiments were performed using Waters HDX with a LEAP system (Waters, Tokyo, Japan), as previously reported [30]. The antigen (recombinant human MDA5) and antibody (anti-human MDA5 monoclonal antibody clone H46) complexes (hereby antigen + antibody complex) were prepared by mixing equal amounts of 160 μM antigen solution and 160 μM antibody solution suspended in 50 mM Tris-HCl, 150 mM NaCl, 1 mM EDTA, 0.01 % CHAPS, and 1 mM TCEP (pH 8.0). Moreover, 80 μM protein solutions (antigen, antigen + antibody complex) was diluted 20-fold with 50 mM Tris-HCl, 150 mM NaCl, 1 mM EDTA, 0.01 % CHAPS, and 1 mM TCEP (pH 8.0) and incubated at 20 °C for various hydrogen/deuterium exchange time points (0.5, 1, 10, 60, and 240 min). The exchange reaction was quenched by dropping the pH to 2.4 with mixing equal volume of 100 mM phosphate, 4 M guanidinium chloride, 0.5 M TCEP (pH 2.3). The quenched samples (100 pmol) were immediately injected, desalted, and separated online using a Waters UPLC system based on the NanoACQUITY ™ platform. The online digestion was performed for over 6 min in water containing 0.05 % formic acid at 4 °C at a flow rate of 50 μL/min. The digested peptides were trapped on an ACQUITY UPLC BEH C18 1.7 μm peptide trap (Waters) maintained at 0 °C and desalted with water and 0.1 % formic acid. Flow was diverted by a switching valve, and the trapped peptide fragments were eluted at 40 μL/min onto a column of 1 × 100 mm (C18 1.7 μm, ACQUITY UPLC BEH, Waters) held at 0 °C, with a 9 min linear acetonitrile gradient (8–40 %) containing 0.1 % formic acid. The eluate was directed into a mass spectrometer (Synapt HD, Waters) with electrospray ionization and lock mass correction (using glu-fibrinogen peptide B). Mass spectra were transformed using MassLynx (Waters) and acquired over an m/z range of 100–2000. Pepsin fragments were identified using a combination of exact mass and MS/MS, aided by the ProteinLynx Global SERVER (PLGS, Waters). Peptide deuterium levels were determined using DynamX 3.0 (Waters). Peptides that were significantly different between the antigen and antigen + antibody complexes were evaluated by creating volcano plots with 99 % confidence intervals (CIs) for the degree of deuterium exchange, using Welch's t-test. The mass difference in hydrogen-deuterium exchange (ΔHX) for each peptide at each deuterium exchange time is calculated as follows.

$$\Delta HX = \mathrm{m}_{\mathrm{sample1}} - \mathrm{m}_{\mathrm{sample2}}$$

Sample 1 shows the antigen + antibody (recombinant human MDA5 and anti-human MDA5 monoclonal antibody clone H46) complex and sample 2 shows the antigen (recombinant human MDA5) protein.

2.10. Surface antigen and intracellular analysis by flow cytometry

Purified anti-human MDA5 mAbs (clones H5 and H27) were conjugated with fluorescein using a Fluorescein Labeling Kit-NH_2 ® (Dojindo, Kumamoto, Japan). Flow cytometric analysis was performed using BD FACSLyric™ (BD, Tokyo, Japan). Four-color analysis was performed for surface and intracellular analyses. Isolated PBMCs were stimulated with or without poly I:C as described above. For intracellular cellular analysis, the cells were treated with 1 % paraformaldehyde and 0.1 % saponin. Cells were stained with fluorescein conjugated anti-human MDA5 mAbs (clones H5 or H27), PE/Cy7-anti-human CD4 mAb (clone OKT4, Biolegend, Tokyo, Japan), APC-anti-human CD8a mAb (Clone RPA-T8, Biolegend), PE-anti-human CD16 mAb (clone 3G8, Biolegend), anti-human CD19 (clone HIB19, Biolegend), and/or control isotype matched mouse Immunoglobulin (Biolegend), as we have reported previously [31,32]. The lymphocyte population was gated for analysis.

2.11. Statistical analysis

Results are expressed as means ± standard error of the mean (SEM). Non-parametric tests (Wilcoxon/Kruskal–Wallis test) were used to compare the differences between groups. Correlations were analyzed using simple regression. Statistical significance was set at $P < 0.05$. significance. All analyses were performed using the JMP Pro software (version 17.0.0; SAS Institute, Cary, NC, USA).

2.12. Ethical issues

This study was approved by the Institutional Review Board of Kurume University Hospital (approval date: July 31, 2019; approval number:19090) and performed in accordance with the 2013 Declaration of Helsinki. Informed consent for participation in this study was obtained from all participants. All animal procedures were approved by the Committee on the Ethics of Animal Experiments at Kurume University (Approval No. 2022-083, 2022-084, 2022-085). Animal care was performed in accordance with the procedures

outlined in the "Principles of Laboratory Animal Care (National Institutes of Health Publication 86-23, revised 1985). All efforts were made to minimize suffering of the animals used in this study.

3. Results

3.1. Anti-human MDA5 mAb (H46) recognizes a peptide derived from the helicase domain of human MDA5

We established five anti-human MDA5 monoclonal antibodies (clones H5 [mouse IgG1], H27 [mouse IgG1], H46 [mouse IgG2b], H77 [mouse IgG2b], and H85 [mouse IgG1]). Anti-human MDA5 mAbs (clones H5 and H27) were used for western blotting and intracellular flow cytometric staining. Western blot analysis showed that HEK293T cells strongly expressed the approximately 120 kDa MDA5 protein (data not shown). HEK293T cells were transfected with pEF-Flag-human MDA5 or pEF-Flag-mouse MDA5 vectors. Human MDA5 was immunoprecipitated using all anti-MDA5 mAb clones and an anti-FLAG M2 antibody but not with normal mouse IgG. In contrast, mouse MDA5 was not immunoprecipitated by the anti-MDA5 mAb clones (Fig. 1), demonstrating the specificity of the anti-human MDA5 clones.

We performed hydrogen deuterium exchange mass spectrometry to examine the antigen (recombinant human MDA5) and antibody (anti-human MDA5 monoclonal antibody clone H46) complexes, as previously reported [30]. In this study, we analyzed 425 peptides, covering 96.7 % of human MDA5 (Table 1). Statistical analysis using a volcano plot is shown in Fig. 2. A positive ΔHX plot indicates a decrease in deuterium exchange degree with the addition of antibody, i.e., interaction sites, while a negative ΔHX plot indicates an increase in the deuterium exchange degree with the addition of the antibody, as reported [30]. Five plots in the region enclosed by the red dotted line ($\Delta HX < -0.4978$ or $\Delta HX < 0.4978$ and p-value < 0.01) are those with significant differences at the 99 % confidence interval. Table 2 shows the list of 5 peptides, the deuterium exchange times, ΔHX, and *p*-value with significant differences at the 99 % confidence interval, as described above. The peptide with a start point of 417(Q) and an end point of 426(L) (sequence QILENSLLNL) was considered the region where the degree of deuterium exchange decreased the most because of the addition of the anti-MDA5 monoclonal antibody clone H46 (Table 1). Taken together, hydrogen deuterium exchange mass spectrometry showed that clone H46 bound to the peptide (415QILENSLLNL424) derived from the helicase domain of human MDA5 (GenBank accession no. AF095844).

3.2. Characteristics of MDA5 expression in human tissues

To study mRNA levels of MDA5 in normal human tissues. Repeated analyses revealed that MDA5 mRNA was constitutively expressed in the lung, spleen, pancreas, and placenta, and was weakly expressed in the muscle. The relative mRNA expression of MDA5 per β-actin in various tissues in the two RT-qPCR experiments is shown in Fig. 3A. We performed western blotting to evaluate MDA5 protein expression using an MDA5 mAb (clone H27). Normal lung and lung cancer tissues were obtained from two patients (Patients 1 and 2) with squamous lung cancer. Western blot analysis showed that PBMCs, normal lung tissues, and lung cancer tissues expressed MDA5. The molecular size of human MDA5 is approximately 120 kDa, as previously reported [33]. Three cancer cell lines, 293T, A549, and HeLa, have also expressed MDA5 at approximately 120 kDa (data not shown). Moreover, we found a weak band of MDA5 protein of approximately 60 kDa in PBMCs and normal and cancerous lung tissues. Representative Western blot analysis results are shown in Fig. 3B.

Next, we analyzed the MDA5 protein expression in normal lungs. Immunohistochemical analysis using an in-house anti-MDA5 mAb (clone H27) also showed that epithelial and vascular endothelial cells weakly expressed MDA5. Interestingly, alveolar macrophages moderately expressed MDA5 protein (upper panel, Fig. 4). We obtained normal tonsil and pancreatic tissues and performed

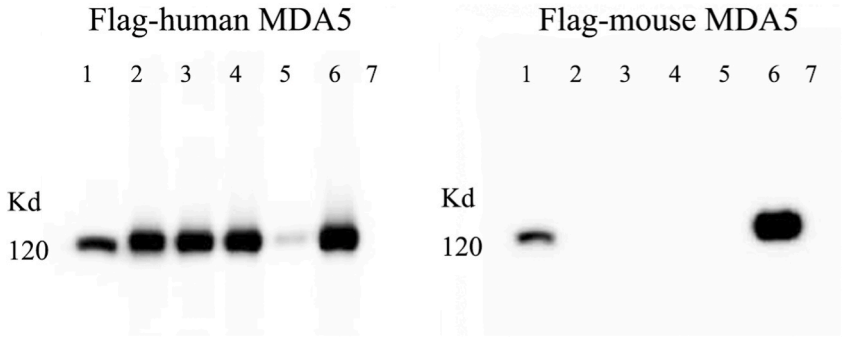

Fig. 1. Immunoprecipitation shows anti-human MDA5 monoclonal antibodies (mAbs) recognize human but not mouse MDA5 protein. The HEK293T cells were transfected with Flag-human MDA5 cDNA (left panel). HEK293T cells were transfected with Flag-mouse MDA5 cDNA (right panel). Diluted whole-cell extract of Flag-human MDA5 overexpressing HEK293T cells (line 1, left) or Flag-mouse MDA5 overexpressing HEK293T cells (line 1, right) were used as positive controls. Immunoprecipitation was performed using four different anti-human MDA5 mAbs (clones H27 [no. 2], H46 [no. 3], H77 [no. 4], and H85 [no. 5]), anti-Flag M2 antibody [no. 6], and control normal mouse IgG [no. 7]. Western blotting was performed using anti-Flag M2 antibody.

Table 1
We analyzed 425 peptides, covering 96.7 % of human MDA5 by hydrogen deuterium exchange mass spectrometry. The peptide with a start point of 417(Q) and an end point of 426(L) (no. 169, sequence QILENSLLNL) is shown in bold.

Sequence	Start	End
1. YSTDENF	7	13
2. FRYLISCFRARVK	13	25
3. RYLISCFRARV	14	24
4. YIQVEPVL	27	34
5. YIQVEPVLDYLTFL	27	40
6. IQVEPVLDYLTFL	28	40
7. PVLDYL	32	37
8. PVLDYLTFLP	32	41
9. LDYLTF	34	39
10. DYLTFLPAEVKEQIQRTV	35	52
11. YLTFLPAE	36	43
12. YLTFLPAEVK	36	45
13. TFLPAEVKEQIQRTVATSGNMQA	38	60
14. PAEVKEQIQRT	41	51
15. PAEVKEQIQRTVA	41	53
16. PAEVKEQIQRTVATSGNMQA	41	60
17. VKEQIQRTVATSGNM	44	58
18. VKEQIQRTVATSGNMQA	44	60
19. KEQIQRTVATSGNMQAVELLLSTLEK	45	70
20. QIQRTVATSGNM	47	58
21. IQRTVATSGN	48	57
22. QRTVATSGNM	49	58
23. VATSGN	52	57
24. ATSGNMQAVELL	53	64
25. GNMQAVELLLSTLEKGVWH	56	74
26. LLSTLEKGVWHLGWTRE	64	80
27. LSTLEKGVWHLGWTRE	65	80
28. STLEKGVWHLGWTRE	66	80
29. TLEKGVWHLGWTR	67	79
30. LEKGVWHLGW	68	77
31. LEKGVWHLGWTR	68	79
32. LEKGVWHLGWTRE	68	80
33. EKGVWHLGWTRE	69	80
34. GVWHLGWTRE	71	80
35. VWHLGWTREFVE	72	83
36. EFVEALR	80	86
37. EFVEALRR	80	87
38. FVEALRRT	81	88
39. VEALRRTGSP	82	91
40. ALRRTGSPLA	84	93
41. LRRTGSPLAA	85	94
42. RRTGSPLAARY	86	96
43. RRTGSPLAARYMNPEL	86	101
44. TGSPLAARYM	88	97
45. GSPLAA	89	94
46. GSPLAAR	89	95
47. TDLPSP	102	107
48. TDLPSPSF	102	109
49. TDLPSPSFE	102	110
50. LPSPSF	104	109
51. ENAHDEY	110	116
52. NAHDEY	111	116
53. AHDEYLQLLNLLQPT	112	126
54. HDEYLQLLNLLQ	113	124
55. QLLNLLQPTLV	118	128
56. LLNLLQPTLVD	119	129
57. LNLLQPTL	120	127
58. LNLLQPTLVD	120	129
59. NLLQPTL	121	127
60. LVRDVL	132	137
61. RDVLDKCMEEEL	134	145
62. EEELLTIEDRNRI	142	154
63. LTIEDRNRIAAAENNGNESG	146	165
64. LTIEDRNRIAAAENNGNESGVRELL	146	170
65. DRNRIAAAEN	150	159
66. DRNRIAAAENNGNESGVRE	150	168

(*continued on next page*)

Table 1 (*continued*)

Sequence	Start	End
67. AENNGNESGVRELL	157	170
68. LLKRIVQKENW	169	179
69. KENWFSAFLNVL	176	187
70. FSAFLN	180	185
71. FSAFLNVLRQTGNNE	180	194
72. FLNVLRQTGNN	183	193
73. FLNVLRQTGNNELV	183	196
74. LNVLRQTGNN	184	193
75. LNVLRQTGNNEL	184	195
76. VLRQTGNNELVQEL	186	199
77. LRQTGNNELVQ	187	197
78. RQTGNNEL	188	195
79. LVQELT	195	200
80. VQELTGSD	196	203
81. VQELTGSDCSESNA	196	209
82. SNAEIENLSQVD	207	218
83. IENLSQVDGPQVEEQLLSTTVQPNL	211	235
84. SQVDGP	215	220
85. SQVDGPQVE	215	223
86. SQVDGPQVEE	215	224
87. SQVDGPQVEEQL	215	226
88. SQVDGPQVEEQLL	215	227
89. VDGPQVE	217	223
90. VDGPQVEEQL	217	226
91. DGPQVE	218	223
92. GPQVEEQL	219	226
93. VEEQLLSTTVQPNL	222	235
94. EQLLSTTVQPNLEK	224	237
95. LSTTVQPNL	227	235
96. LSTTVQPNLE	227	236
97. STTVQPNL	228	235
98. TVQPNLE	230	236
99. EKEVWGMENNSSESSF	236	251
100. FADSSV	251	256
101. ADSSVVSE	252	259
102. SVVSESDTSL	255	264
103. VSESDTSL	257	264
104. SESDTSL	258	264
105. TSLAEGSVS	262	270
106. TSLAEGSVSCL	262	272
107. LAEGSV	264	269
108. AEGSVSC	265	271
109. AEGSVSCL	265	272
110. VSCLDES	269	275
111. LDESLG	272	277
112. DESLGHNSNMG	273	283
113. SLGHNSNMGS	275	284
114. ENVAARASP	296	304
115. NVAARA	297	302
116. AARASP	299	304
117. ARASPEPEL	300	308
118. PELQLRPYQMEVAQP	306	320
119. ELQLRPYQME	307	316
120. ELQLRPYQMEVAQPALE	307	323
121. QMEVAQPALE	314	323
122. MEVAQP	315	320
123. MEVAQPALEGKNII	315	328
124. EVAQPAL	316	322
125. EVAQPALEGKN	316	326
126. EVAQPALEGKNII	316	328
127. VAQPAL	317	322
128. VAQPALEGKN	317	326
129. VAQPALEGKNIIIC	317	330
130. PALEGKN	320	326
131. ALEGKNIIICLP	321	332
132. IIICLPTGSGKTRVAV	327	342
133. IICLPTGSGKT	328	338
134. CLPTGSGKTRVAV	330	342
135. LPTGSGKTRVAV	331	342

(*continued on next page*)

Table 1 (*continued*)

Sequence	Start	End
136. PTGSGKTRVAV	332	342
137. PTGSGKTRVAVY	332	343
138. TGSGKTRVAVY	333	343
139. TGSGKTRVAVYI	333	344
140. SGKTRV	335	340
141. GKTRVA	336	341
142. VAVYIA	340	345
143. YIAKDHLDKKKKASEPGKVIVL	343	364
144. IAKDHLDKKKKASEPGKVIVL	344	364
145. DKKKKASEPGKVIVL	350	364
146. VNKVLL	365	370
147. VNKVLLVEQLFRKEFQP	365	381
148. LFRKEFQPFL	374	383
149. FRKEFQPFL	375	383
150. FRKEFQPFLKK	375	385
151. FRKEFQPFLKKWYRVIG	375	391
152. FRKEFQPFLKKWYRVIGL	375	392
153. KKWYRVIGLSGDTQL	384	398
154. KKWYRVIGLSGDTQLK	384	399
155. WYRVIGLSGDTQL	386	398
156. YRVIGLSGDTQL	387	398
157. RVIGLSGDTQ	388	397
158. IGLSGDTQLKI	390	400
159. GLSGDTQLKI	391	400
160. SGDTQL	393	398
161. LKISFPEVVKSCDIII	398	413
162. KISFPE	399	404
163. ISFPEVVKSC	400	409
164. ISFPEVVKSCD	400	410
165. PEVVKSCD	403	410
166. PEVVKSCDIIISTA	403	416
167. EVVKSCD	404	410
168. VKSCDIIISTAQ	406	417
169. QILENSLLNL	**417**	**426**
170. LLNLEN	423	428
171. LNLENGEDAG	424	433
172. LNLENGEDAGVQ	424	435
173. NLENGEDAGVQ	425	435
174. ENGEDAGVQL	427	436
175. DAGVQL	431	436
176. DAGVQLSDFSLI	431	442
177. DAGVQLSDFSLIIID	431	445
178. AGVQLSD	432	438
179. AGVQLSDFSLIIID	432	445
180. GVQLSDFSLIIIDECHHTNKEAVYN	433	457
181. LSDFSLIIIDEC	436	447
182. SDFSLIIID	437	445
183. DFSLII	438	443
184. IIIDECHHTNKEAV	442	455
185. IIIDECHHTNKEAVYNN	442	458
186. IIIDECHHTNKEAVYNNIMRH	442	462
187. IDECHHTNKEAV	444	455
188. IDECHHTNKEAVYNNIMRHYLMQ	444	466
189. TNKEAVYN	450	457
190. NKEAVYNNIMR	451	461
191. YNNIMRHYLM	456	465
192. IMRHYLMQKLKNNRL	459	473
193. IMRHYLMQKLKNNRLKKENKPVIPLPQILGL	459	489
194. MQKLKNNRLKKENKPVIPLPQILGL	465	489
195. QKLKNNRLKKENKPVIPLPQILGL	466	489
196. KLKNNRLKKENKPVIPLPQILGL	467	489
197. LKKENKPVIPLPQILGLTASP	473	493
198. KKENKPVIPLPQILGL	474	489
199. ENKPVIPLPQI	476	486
200. PQILGL	484	489
201. PQILGLTA	484	491
202. PQILGLTASP	484	493
203. LGLTASPGVGGATKQAKAE	487	505
204. GLTASPG	488	494

(*continued on next page*)

Table 1 (*continued*)

Sequence	Start	End
205. GLTASPGVGG	488	497
206. LTASPGVGGA	489	498
207. TASPGVGGAT	490	499
208. TASPGVGGATKQAKAEE	490	506
209. TASPGVGGATKQAKAEEHILKL	490	511
210. SPGVGGATKQ	492	501
211. SPGVGGATKQAKAEE	492	506
212. SPGVGGATKQAKAEEHILKL	492	511
213. PGVGGAT	493	499
214. PGVGGATKQAKAEE	493	506
215. PGVGGATKQAKAEEH	493	507
216. PGVGGATKQAKAEEHILKL	493	511
217. GVGGATKQAKAEEH	494	507
218. GGATKQAKAEEHILKL	496	511
219. TKQAKAEEHILKLCANL	499	515
220. AKAEEHILKLCANLDAFTIKTV	502	523
221. KAEEHILKLCANLD	503	516
222. EEHILKL	505	511
223. KLCANLDAFT	510	519
224. CANLDA	512	517
225. FTIKTVKENL	518	527
226. FTIKTVKENLDQL	518	530
227. TIKTVKENL	519	527
228. TVKENLDQLKNQ	522	533
229. NLDQLKNQIQEPCKKFAIA	526	544
230. DQLKNQIQEPCKKFAIADATREDPFKEKL	528	556
231. EPCKKFA	536	542
232. PCKKFAIADAT	537	547
233. AIADAT	542	547
234. DATREDPFKEKL	545	556
235. ATREDPFKEKL	546	556
236. ATREDPFKEKLLE	546	558
237. TREDPFKEKL	547	556
238. IMTRIQT	559	565
239. MTRIQTYCQMSPMSDFGTQPY	560	580
240. MTRIQTYCQMSPMSDFGTQPYE	560	581
241. RIQTYC	562	567
242. YCQMSPMSD	566	574
243. YCQMSPMSDF	566	575
244. CQMSPMSD	567	574
245. CQMSPMSDF	567	575
246. MSPMSDF	569	575
247. SPMSDF	570	575
248. SPMSDFGTQPYEQW	570	583
249. FGTQPYEQ	575	582
250. GTQPYEQ	576	582
251. GTQPYEQW	576	583
252. TQPYEQW	577	583
253. PYEQWAIQMEKKA	579	591
254. AIQMEKKAAKKG	584	595
255. EKKAAK	588	593
256. ERVCAEHLRKYNEALQIND	599	617
257. AEHLRKYNEALQINDT	603	618
258. HLRKYNEALQIN	605	616
259. HLRKYNEALQIND	605	617
260. RMIDAY	620	625
261. YTHLET	625	630
262. FYNEEKDK	631	638
263. FYNEEKDKKF	631	640
264. YNEEKDKKFAVIEDDSDEGGDDE	632	654
265. NEEKDKKFAVIEDDSDEGGDDEY	633	655
266. KDKKFA	636	641
267. DDEYCDGDEDEDDLKKPLKLDETDR	652	676
268. YCDGDEDEDDLKKPLKL	655	671
269. YCDGDEDEDDLKKPLKLDETDRF	655	677
270. DEDEDDLKKPLKL	659	671
271. EDEDDLKKPLK	660	670
272. DEDDLKKPLKL	661	671
273. DEDDLKKPLKLDE	661	673

(*continued on next page*)

Table 1 (*continued*)

Sequence	Start	End
274. DDLKKPLKL	663	671
275. DLKKPLKL	664	671
276. LKKPLKL	665	671
277. DETDRF	672	677
278. TDRFLM	674	679
279. DRFLMTLF	675	682
280. DRFLMTLFFENNKMLKRLAENPEYENEKLT	675	704
281. MTLFFE	679	684
282. LFFENNKM	681	688
283. LFFENNKMLKRLAENPEYE	681	699
284. FFENNKM	682	688
285. FFENNKMLKRLAENPEYE	682	699
286. FFENNKMLKRLAENPEYENEKL	682	703
287. FFENNKMLKRLAENPEYENEKLTKLRNTIM	682	711
288. FENNKMLKRLAENPEYENEKL	683	703
289. FENNKMLKRLAENPEYENEKLTKLRNTIM	683	711
290. LKRLAENPEYENEKL	689	703
291. LAENPEYENEKL	692	703
292. LAENPEYENEKLTKLRNTIMEQYTRTE	692	718
293. ENPEYENEKLTK	694	705
294. TKLRNTIM	704	711
295. TKLRNTIMEQ	704	713
296. TKLRNTIMEQYT	704	715
297. IMEQYTRTEESAR	710	722
298. EQYTRTEESARG	712	723
299. QYTRTEESARGIIF	713	726
300. TRTEESARGI	715	724
301. ESARGIIFTKTRQ	719	731
302. SARGII	720	725
303. SARGIIF	720	726
304. SARGIIFTKTRQSAYALSQWIT	720	741
305. IIFTKTRQSAYALS	724	737
306. TKTRQSAYAL	727	736
307. TKTRQSAYALSQ	727	738
308. QSAYALSQWI	731	740
309. YALSQW	734	739
310. ITENEKFAEVGV	740	751
311. TENEKF	741	746
312. TENEKFAEVG	741	750
313. KFAEVGVKAHHLIGAG	745	760
314. AEVGVKAHHL	747	756
315. AEVGVKAHHLIGAGHSSE	747	764
316. AEVGVKAHHLIGAGHSSEF	747	765
317. EVGVKAHHLIGAGHSSE	748	764
318. VGVKAH	749	754
319. VGVKAHHLIGAGHSSE	749	764
320. GVKAHHLIGAGHS	750	762
321. GVKAHHLIGAGHSS	750	763
322. GVKAHHLIGAGHSSE	750	764
323. GVKAHHLIGAGHSSEFKPM	750	768
324. HLIGAG	755	760
325. IGAGHS	757	762
326. FKPMTQN	765	771
327. NEQKEVISKF	771	780
328. QKEVISKFRT	773	782
329. QKEVISKFRTGKINL	773	787
330. SKFRTGKINLLIATTVAEEGLDIKEC	778	803
331. KFRTGK	779	784
332. KFRTGKINLLIATTVAE	779	795
333. RTGKINLL	781	788
334. TGKINL	782	787
335. LLIATT	787	792
336. LIATTV	788	793
337. ATTVAE	790	795
338. ATTVAEEGLD	790	799
339. ATTVAEEGLDIKE	790	802
340. VAEEGLD	793	799
341. EEGLDIKECNIVIR	795	808
342. EEGLDIKECNIVIRYG	795	810

(*continued on next page*)

Table 1 (*continued*)

Sequence	Start	End
343. ECNIVIRYGLVTNEI	802	816
344. IVIRYGL	805	811
345. IVIRYGLVTNE	805	815
346. IVIRYGLVTNEIAMVQ	805	820
347. TNEIAMVQARGRA	813	825
348. TNEIAMVQARGRAR	813	826
349. ARGRARADESTYV	821	833
350. RARADESTYVLVAHSGSGVIEHETVN	824	849
351. RADESTYVLV	826	835
352. RADESTYVLVAHSG	826	839
353. ADESTYVLVAHSGSGV	827	842
354. ESTYVLVAHSGSGVIEHE	829	846
355. YVLVAHSGSGVIEHETVND	832	850
356. VLVAHSGSGV	833	842
357. VAHSGSGVI	835	843
358. VAHSGSGVIEHETVND	835	850
359. AHSGSGVIEH	836	845
360. AHSGSGVIEHETVND	836	850
361. HSGSGVIEHE	837	846
362. SGSGVIEHETVNDFRE	838	853
363. GSGVIEHETV	839	848
364. SGVIEH	840	845
365. SGVIEHETVND	840	850
366. GVIEHETVND	841	850
367. NDFREKMMYKAIHCVQNMK	849	867
368. DFREKMMYKAIHCVQNMKP	850	868
369. FREKMMYKAIHCVQ	851	864
370. FREKMMYKAIHCVQNMKPEE	851	870
371. YKAIHCVQNMKPEE	857	870
372. KAIHCVQNMKPEE	858	870
373. YAHKILE	871	877
374. YAHKILEL	871	878
375. AHKILELQMQSIMEKKMKTK	872	891
376. AHKILELQMQSIMEKKMKTKRNIAKHYK	872	899
377. LQMQSIMEKK	878	887
378. MQSIMEKKMKTK	880	891
379. SIMEKKM	882	888
380. NIAKHYKNNPSL	893	904
381. PSLITF	902	907
382. SLITFLCKNCSVL	903	915
383. SLITFLCKNCSVLACSG	903	919
384. LITFLCKNCSV	904	914
385. ITFLCKNCSVL	905	915
386. ITFLCKNCSVLA	905	916
387. FLCKNCSVLACSGE	907	920
388. LCKNCSVL	908	915
389. LCKNCSVLACSG	908	919
390. CKNCSVL	909	915
391. KNCSVLACSG	910	919
392. VLACSGEDIHVIEK	914	927
393. LACSGED	915	921
394. ACSGEDIHVIE	916	926
395. DIHVIE	921	926
396. DIHVIEKMHHVNMT	921	934
397. IHVIEKMHHVNM	922	933
398. IHVIEKMHHVNMTPEF	922	937
399. KMHHVNMTPEF	927	937
400. FKELYI	937	942
401. YIVRENKALQKKCAD	941	955
402. VRENKALQKKCAD	943	955
403. ENKALQKKCADYQ	945	957
404. ALQKKCADYQINGEIICKCGQAWGTMMV	948	975
405. ADYQINGEIICKCGQ	954	968
406. INGEIIC	958	964
407. IICKCGQAWGTM	962	973
408. GTMMVHKGLDLPCLKIRNFVVVFKNNS	971	997
409. MVHKGLDL	974	981
410. MVHKGLDLPCL	974	984
411. MVHKGLDLPCLKIRN	974	988

(*continued on next page*)

Table 1 (*continued*)

Sequence	Start	End
412. VHKGLDLPCL	975	984
413. HKGLDL	976	981
414. HKGLDLPCLK	976	985
415. NFVVVF	988	993
416. VVVFKNNSTKKQYKKWVEL	990	1008
417. VVFKNNSTKKQYKKWVEL	991	1008
418. VFKNNSTKKQYKKWVEL	992	1008
419. FKNNST	993	998
420. KNNSTKKQYKKWVEL	994	1008
421. STKKQY	997	1002
422. QYKKWVELPITFPN	1001	1014
423. PITFPNL	1009	1015
424. PITFPNLD	1009	1016
425. PITFPNLDY	1009	1017

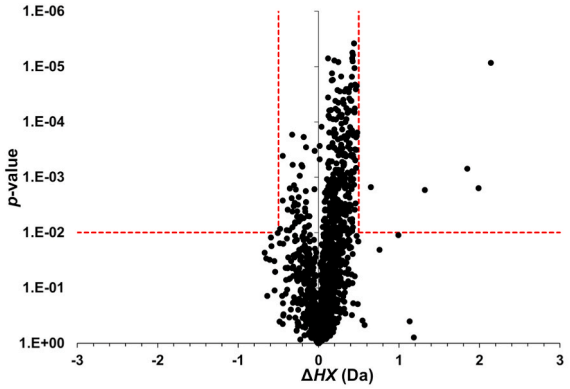

Fig. 2. Volcano plot showing the mass difference in hydrogen-deuterium exchange (Δ*HX*) and *p*-value at each deuterium exchange time for peptides detected by hydrogen deuterium exchange mass spectrometry experiments. Five plots in the region enclosed by the red dotted line (ΔHX < -0.4978 or ΔHX<0.4978 and p-value <0.01) are those with significant differences at the 99 % confidence interval.

Table 2
Start and end points and deuterium exchange times of 5 peptides with significant differences in the analysis by Volcano plot and the difference of their deuterium exchange degree and p-value at the 99 % confidence interval.

Peptide No.	Start	End	Exchange time (min.)	Δ*HX* (Da)	*p*-value
1	417	426	0.5	0.6458	0.002
2	417	426	1	1.318	0.002
3	417	426	10	1.847	0.001
4	417	426	60	1.9857	0.002
5	417	426	240	2.1403	0.001

immunohistochemical analysis of MDA5 protein expression. MDA5 protein was strongly expressed in the cytoplasm of lymphoid cells in the tonsils (lower right panel, Fig. 4) and acinar cells of the pancreas (lower left panel, Fig. 4).

3.3. Soluble MDA5 protein in sera

We tested MDA5 protein in the sera of 32 healthy donors using two human MDA5 mAbs (clones H27 and H46). Using electrochemiluminescence in a MESOSCALE DISCOVERY® assay system, the dynamic range of this assay system ranges approximately from 100 pg/mL through 250 ng/mL. We found that soluble MDA5 protein was detectable in sera from 14 of the 32 healthy donors (3314 ± 7215 pg/mL, Fig. 5). Moreover, the level of soluble MDA5 protein in the sera of the three donors was >10 ng/ml. In contrast, soluble MDA5 was not detected in the urine of six donors; however, soluble MDA5 protein was detectable in the serum of two of these six urine donors. Next, we tested the MDA5 protein levels in the sera of 31 patients with DM. We found that soluble MDA5 protein was detectable in sera from 26 of the 31 DM patients (635 ± 791 pg/mL, Fig. 5). The mean levels of soluble MDA5 protein in the sera of 32 healthy donors were higher than those in the sera of 31 patients with DM; however, the difference was not significant.

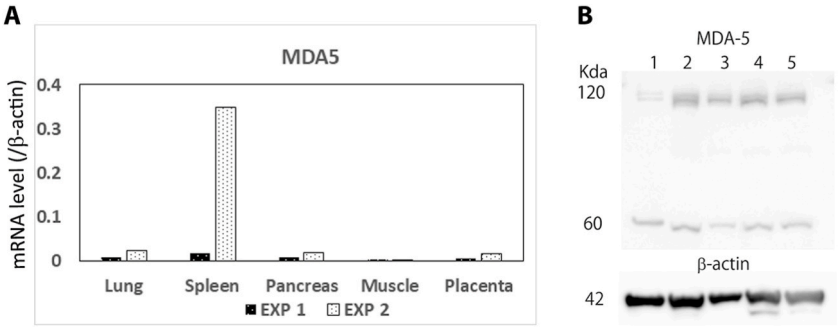

Fig. 3. MDA5 mRNA and protein expression in the human lungs. (A) Complementary DNAs (cDNAs) isolated from normal human tissues (lung, spleen, pancreas, muscle, and placenta). Two different real-time quantitative PCRs (RT-qPCR) were performed. Mean relative expression was calculated using the comparative threshold cycle method. Relative mRNA expression of MDA5 per β-actin is shown in Y-axis. (B) PBMCs were obtained from a healthy donor. Normal lungs and cancerous lungs were obtained from a 67-year-old male patient (patient 1) with squamous cell carcinoma (SCC) of the lung. Western blot analysis of PBMCs, normal lungs, and cancerous lungs using mouse anti-human MDA5 mAb (H27) and anti-β-actin mAb.
1. PBMCs (100 ng/lane). 2. Normal lung (left lung, S6, 100 ng/lane) (patient 1). 3. Normal lung (left lung, S8, 100 ng/lane) (patient 1). 4. Normal lungs (left lung S10, 100 ng/lane) (patient 1). 5. Lung cancer (100 ng/lane) (patient 1).

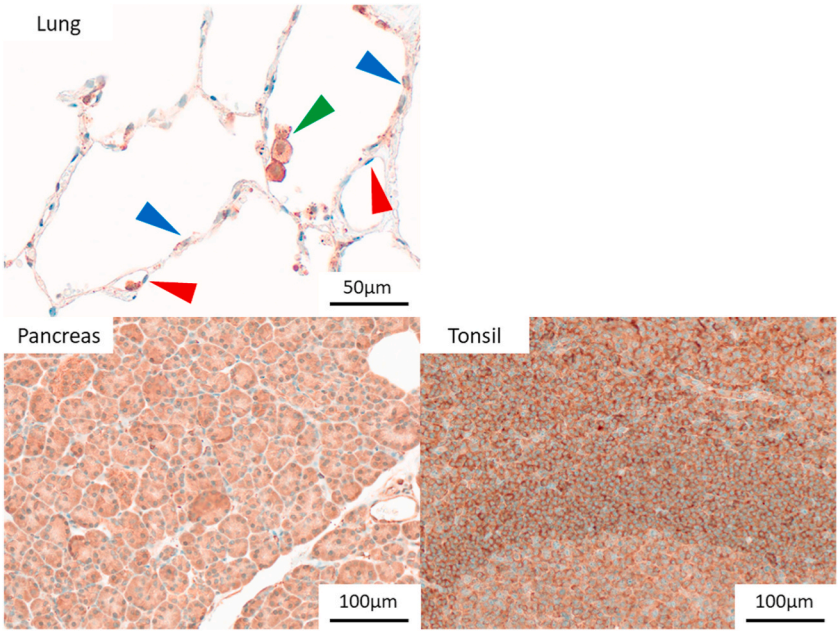

Fig. 4. Immunohistochemical analysis of MDA5 expression in tissues. Immunohistochemical analysis with our established mouse anti-human MDA5 mAb (clone H27) in the normal lung (upper panel), normal tonsil (lower left), and pancreas (lower right) was performed with mouse anti-human MDA5 mAb (clone H27).
Green arrowhead: Macrophages. Blue arrowhead: Alveolar epithelial cells. Red arrowhead: Vascular endothelial cells.

3.4. Characteristics of soluble MDA5 protein

As MDA5 is a viral receptor, we hypothesized that soluble MDA5 could be obtained through the stimulation of immune cells. We hypothesized that PBMCs would produce soluble MDA5. Subsequently, PBMCs were isolated from four healthy donors, suspended in cold PBS at 2×10^6 cells/mL, and stimulated with 250 μg/mL poly I:C at 37 °C to activate MDA5 [2]. Five experiments were conducted. Supernatants were harvested at various time points (0, 15, 1, and 2h). The levels of MDA5 protein in the supernatants of PBMCs without poly I:C were 0 ± 0 pg/mL at 0 min, 493 ± 486 pg/mL at 15 min, 262 ± 224 pg/mL at 1 h, and 111 ± 166 pg/mL at 2 h. The levels of MDA5 protein in the supernatants of PBMCs with poly I:C were 0 ± 0 pg/mL at 0 min, 731 ± 593 pg/mL at 15 min, 175 ± 141 pg/mL at 1 h, and 111 ± 157 pg/mL at 2 h. Sandwich immunoassay revealed that MDA5 protein levels increased in the supernatant of PMBCs within 15 min of poly I:C stimulation. However, they were barely detectable after 2 h. Representative data are shown in Fig. 6A. Western blotting showed the same results; MDA5 protein increased in the supernatant of PMBCs within 15 min after poly I:C

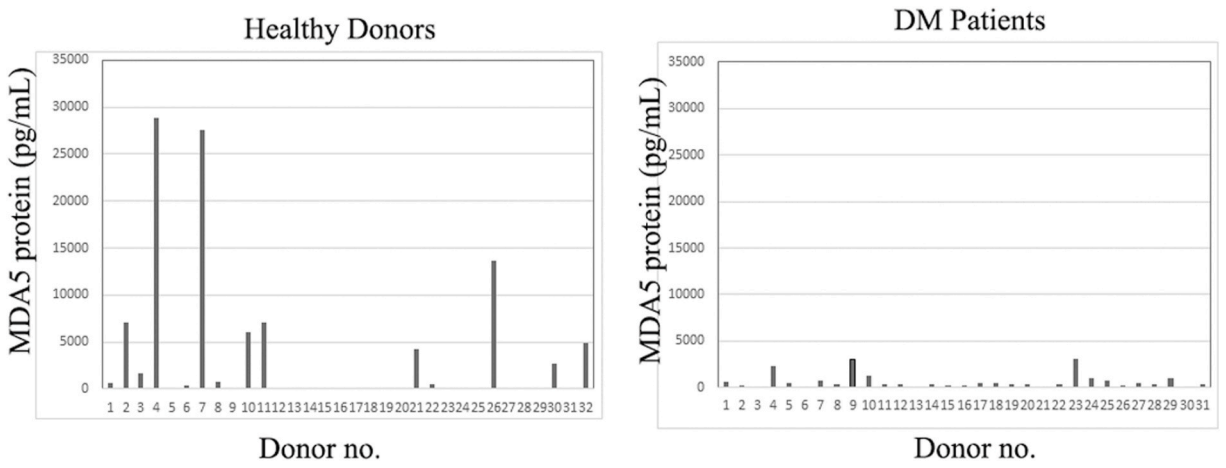

Fig. 5. Serum levels of soluble MDA5 protein. Serum levels of soluble MDA5 were analyzed in 32 healthy donors (left) and 31 patients with DM (right) using an in-house highly sensitive sandwich immunoassay system. Values for MDA 5 protein (pg/mL) are shown on the Y-axis. The sensitivity limit of the assay was 80 pg/mL.

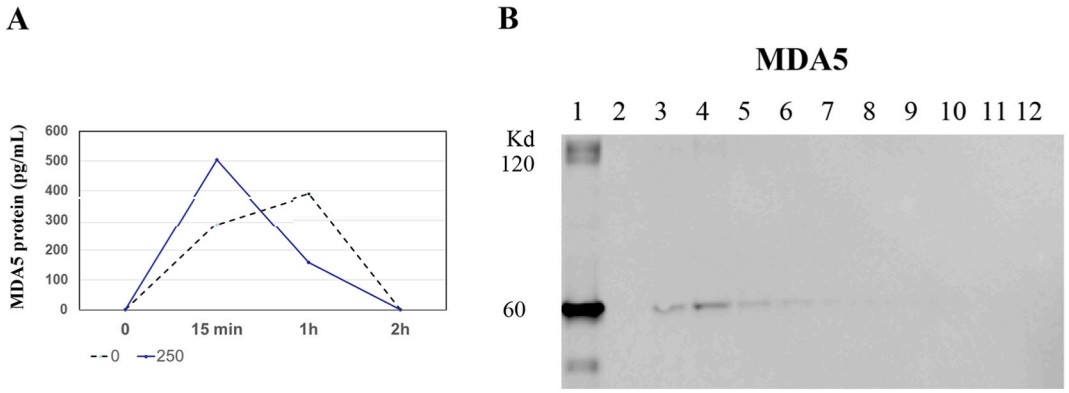

Fig. 6. Characteristics of soluble human MDA5 protein (A) Peripheral blood nuclear cells (PBMCs) were isolated from peripheral blood. Cells (2×10^6 cells/mL in PBS) were stimulated with or without 250 mg/mL polyinosinic-polycytidylic acid sodium salt (poly I:C) at 37 °C. The level of soluble MDA5 in the supernatants was analyzed. The vales of MDA 5 protein (pg/mL) were shown in the Y-axis. (B) Western blot analysis for the MDA5 protein was perform with mouse anti-human MDA5 mAb (clone H27). 1. Whole PBMC. 2. Supernatant at 0 min. 3. Supernatant at 15 min without stimulation. 4. Supernatant at 15 min with stimulation by poly I:C. 5. Supernatant at 1 h without stimulation. 6. Supernatant at 1 h with stimulation by poly I:C. 7. Supernatant at 2 h without stimulation. 8. Supernatant at 2 h stimulation by poly I:C.

stimulation but was hardly detectable after 2 h. The molecular size of soluble MDA5 was approximately 60 kDa. As described above (Fig. 3B), PBMCs expressed MDA5 protein with molecular weights of approximately 60 and 120 kDa, respectively (Fig. 6B).

4. Discussion

In our study, we demonstrated that the MDA5 protein is present in the serum in a soluble form. Our RT-qPCR study showed that MDA5 mRNA was expressed in various organs of healthy humans, indicating that MDA5 was present in all cells, as previously reported [1]. However, immunohistochemical staining revealed that MDA5 was more strongly expressed in alveolar macrophages than in the alveolar epithelium or vascular endothelium of the lungs. This may be due to phagocytosis of exudate-soluble MDA5 in the alveolar space by alveolar macrophages. Furthermore, we demonstrated that the stimulation of PBMCs elevated soluble MDA5 levels, indicating the strong involvement of immune cells in the formation of soluble MDA5.

The full-length MDA5 (*IFIH1*) cDNA encodes 1025 amino acids [33] with a predicted molecular weight of 116,686.83. Using the newly developed mAbs, we observed two immunoreactive bands of the MDA5 protein with molecular weights of 60 and 120 kDa in PBMCs, normal lungs, and cancerous lung tissues. Here, we showed that the 60 kDa MDA5 protein increased in the supernatant of PBMCs within 15 min of synthetic MDA5 agonist/dsRNA stimulation. Hydrogen/deuterium exchange Mass Spectrometry (HDX-MS) was used to analyze the structural features and dynamic properties of proteins. HDX-MS revealed that an anti-human MDA5 mAb (clone H46) bound to an epitope (415QILENSLLNL424) derived from the helicase domain of the MDA5 protein. These results suggest

that soluble MDA5 proteins containing a helicase domain can be generated by alternative splicing of MDA5 mRNA or digestion of MDA5 protein by proteases in some tissues.

In RNA viruses, dsRNA is generated as a replication intermediate during viral infections. TLR3, which localizes to the endosomal membrane, recognizes viral dsRNA and synthetic dsRNA analogs [34]. As described above, the cytoplasmic proteins RIG-I and MDA5 recognize viral dsRNAs and synthetic dsRNA analogs [2]. Although it is unknown whether soluble MDA5 can bind to dsRNA and/or ssRNA viruses, soluble MDA5 can interfere with the recognition of RNA viruses by TLR3, RIG-I, and MDA5. We are currently investigating this issue to better define the roles of soluble MDA5 proteins.

A multicenter retrospective cohort study of Japanese patients with myositis-associated ILD (JAMI) at 44 centers in Japan showed that the presence of anti-MDA5 antibody is an independent risk factor for DM-ILD mortality, as well as, old age, high CRP, and low peripheral capillary oxygen saturation [35]. Increased levels of Coxsackie B virus antibodies in patients with juvenile DM have been reported previously [36]. Another study reported regional differences in the incidence of anti-MDA5 antibodies in Japanese patients with DM [37]. Therefore, viral infections and environmental factors may contribute to the production of autoantibodies against MDA5. We have recently reported that MDA5 was moderately or strongly expressed in the lungs of patients with DM [22]. In this study, we measured serum levels of MDA5 protein in patients with DM. MDA5 protein was detected in the sera of patients with DM. However, the molecular mechanisms underlying anti-MDA5 antibody production in patients are still unknown.

We examined the subset of cells that expressed MDA5 after stimulation with poly (I: C). We isolated from healthy donors. PBMCs were stimulated with or without poly I:C for 15, 30, 1, or 2 h. We, then, performed surface and intra-cellular staining (ICS) on different subpopulations of cells ($CD4^+$ T cells, $CD8^+$ T cells, $CD16^+$ cells, $CD19^+$ B cells, and $CD56^+$ NK cells) using flow cytometry. In freshly isolated PBMCs, not all cell populations expressed MDA5 on their surfaces, but highly expressed MDA5 protein in the cell cytoplasm. After stimulation with poly I:C, the expression of MDA5 was not altered on the surface or in the cytoplasm (data not shown). These results suggest that the 60 kDa form of MDA5 is present in the cytoplasm.

We found that soluble MDA5 protein was detectable in some sera, but not in the urine of healthy donors. Soluble MDA5 protein was rapidly released from the cytoplasm of the tissues after dsRNA poly I:C stimulation. MDA5 was also detected in the supernatant of PBMCs that were not stimulated with poly I:C. These results suggest 1) RNA viral infection increases the levels of soluble MDA5 protein in sera. 2) PBMCs constitutively release soluble MDA5 from the cytoplasm. 3) Soluble MDA5 protein is released from dying cells. Nonetheless, further analyses are required to confirm these hypotheses. The present study can help understand the role of MDA5 in the recognition of RNA viruses and the development of autoimmune diseases.

Data availability statement

The authors declare that the data supporting the findings of this study are available within the paper. A request for more detailed data should be sent to the corresponding authors with the permission of all authors.

Funding

This work was supported by a Grant-in-Aid for Scientific Research (C) (no. 19K08637, T.H.) from the Ministry of Education, Science, and Sports (Japan) and the Kakihara Science Technology Foundation (Fukuoka, Japan). It was also funded by the Deutsche Forschungsgemeinschaft (German Research Foundation) under Germany's Excellence Strategy-EXC2151-390873048 and TRR237 and by the Deutsche Forschungsgemeinschaft (German Research Foundation) Grant No. 369799452 and Project No. 404459591.

CRediT authorship contribution statement

Masaki Okamoto: Writing – original draft, Conceptualization. **Yoshiaki Zaizen:** Writing – original draft, Validation, Formal analysis, Data curation. **Shinjiro Kaieda:** Data curation. **Takashi Nouno:** Data curation. **Takuma Koga:** Data curation. **Goushi Matama:** Data curation. **Masahiro Mitsuoka:** Data curation. **Jun Akiba:** Data curation. **Shintaro Yamada:** Data curation. **Hiroki Kato:** Funding acquisition, Data curation. **Tomoaki Hoshino:** Writing – original draft, Investigation, Funding acquisition, Conceptualization.

Declaration of competing interest

The authors declare the following financial interests/personal relationships which may be considered as potential competing interests:Tomoaki Hoshino has patent pending to Detecting soluble form of MDA5.

Acknowledgments

The authors are grateful to Dr. Howard A. Young (National Cancer Institute-Frederick) and Dr. Takeshi Kawabe (Tohoku University, Sendai, Japan) for editing our manuscript and Dr. Shigekazu Nagata (Osaka University, Suita, Japan) for providing the pEF-BOS-EX vector.

Appendix A. Supplementary data

Supplementary data to this article can be found online at https://doi.org/10.1016/j.heliyon.2024.e31727.

References

[1] M. Yoneyama, K. Onomoto, M. Jogi, et al., Viral RNA detection by RIG-I-like receptors, Curr. Opin. Immunol. 32 (2015) 48–53.
[2] H. Kato, O. Takeuchi, S. Sato, et al., Differential roles of MDA5 and RIG-I helicases in the recognition of RNA viruses, Nature 441 (2006) 101–105.
[3] Z.B. Zalinger, R. Elliott, K.M. Rose, et al., MDA5 is critical to host defense during infection with murine coronavirus, J. Virol. 89 (2015) 12330–12340.
[4] N.G. Sampaio, L. Chauveau, J. Hertzog, et al., The RNA sensor MDA5 detects SARS-CoV-2 infection, Sci. Rep. 11 (2021) 13638.
[5] M. Yoneyama, T. Fujita, Function of RIG-I-like receptors in antiviral innate immunity, J. Biol. Chem. 282 (2007) 15315–15318.
[6] I.T. Lamborn, H. Jing, Y. Zhang, et al., Recurrent rhinovirus infections in a child with inherited MDA5 deficiency, J. Exp. Med. 214 (2017) 1949–1972.
[7] M. Funabiki, H. Kato, Y. Miyachi, et al., Autoimmune disorders associated with gain of function of the intracellular sensor MDA5, Immunity 40 (2014) 199–212.
[8] H. Onizawa, H. Kato, H. Kimura, et al., Aicardi-Goutieres syndrome-like encephalitis in mutant mice with constitutively active MDA5, Int. Immunol. 33 (2021) 225–240.
[9] T. Shigemoto, M. Kageyama, R. Hirai, et al., Identification of loss of function mutations in human genes encoding RIG-I and MDA5: implications for resistance to type I diabetes, J. Biol. Chem. 284 (2009) 13348–13354.
[10] S. Nejentsev, N. Walker, D. Riches, et al., Rare variants of IFIH1, a gene implicated in antiviral responses, protect against type 1 diabetes, Science 324 (2009) 387–389.
[11] G.I. Rice, Y. Del Toro Duany, E.M. Jenkinson, et al., Gain-of-function mutations in IFIH1 cause a spectrum of human disease phenotypes associated with upregulated type I interferon signaling, Nat. Genet. 46 (2014) 503–509.
[12] H. Oda, K. Nakagawa, J. Abe, et al., Aicardi-Goutieres syndrome is caused by IFIH1 mutations, Am. J. Hum. Genet. 95 (2014) 121–125.
[13] R.D. Sontheimer, Would a new name hasten the acceptance of amyopathic dermatomyositis (dermatomyositis sine myositis) as a distinctive subset within the idiopathic inflammatory dermatomyopathies spectrum of clinical illness? J. Am. Acad. Dermatol. 46 (2002) 626–636.
[14] I. Marie, P.Y. Hatron, S. Dominique, et al., Short-term and long-term outcomes of interstitial lung disease in polymyositis and dermatomyositis: a series of 107 patients, Arthritis Rheum. 63 (2011) 3439–3447.
[15] S. Sato, M. Hirakata, M. Kuwana, et al., Autoantibodies to a 140-kd polypeptide, CADM-140, in Japanese patients with clinically amyopathic dermatomyositis, Arthritis Rheum. 52 (2005) 1571–1576.
[16] N. Yoshida, M. Okamoto, S. Kaieda, et al., Association of anti-aminoacyl-transfer RNA synthetase antibody and anti-melanoma differentiation-associated gene 5 antibody with the therapeutic response of polymyositis/dermatomyositis-associated interstitial lung disease, Respiratory investigation 55 (2017) 24–32.
[17] S. Sakamoto, M. Okamoto, S. Kaieda, et al., Low positive titer of anti-melanoma differentiation-associated gene 5 antibody is not associated with a poor long-term outcome of interstitial lung disease in patients with dermatomyositis, Respiratory investigation 56 (2018) 464–472.
[18] L. Li, Q. Wang, F. Yang, et al., Anti-MDA5 antibody as a potential diagnostic and prognostic biomarker in patients with dermatomyositis, Oncotarget 8 (2017) 26552–26564.
[19] S.L. Zunt, L.V. Burton, L.I. Goldblatt, et al., Soluble forms of Toll-like receptor 4 are present in human saliva and modulate tumour necrosis factor-alpha secretion by macrophage-like cells, Clin. Exp. Immunol. 156 (2009) 285–293.
[20] M.J. Hossain, E. Morandi, R. Tanasescu, et al., The soluble form of toll-like receptor 2 is elevated in serum of multiple sclerosis patients: a novel potential disease biomarker, Front. Immunol. 9 (2018) 457.
[21] A. Bohan, J.B. Peter, Polymyositis and dermatomyositis (first of two parts), N. Engl. J. Med. 292 (1975) 344–347.
[22] Y. Zaizen, M. Okamoto, K. Azuma, et al., Enhanced immune complex formation in the lungs of patients with dermatomyositis, Respir. Res. 24 (2023) 86.
[23] S.I. Takenaka, S. Kaieda, T. Kawayama, et al., IL-38: a new factor in rheumatoid arthritis, Biochemistry and biophysics reports 4 (2015) 386–391.
[24] Y. Kitasato, T. Hoshino, M. Okamoto, et al., Enhanced expression of interleukin-18 and its receptor in idiopathic pulmonary fibrosis, Am. J. Respir. Cell Mol. Biol. 31 (2004) 619–625.
[25] S. Mizushima, S. Nagata, pEF-BOS, a powerful mammalian expression vector, Nucleic Acids Res. 18 (1990) 5322.
[26] M. Yoneyama, M. Kikuchi, K. Matsumoto, et al., Shared and unique functions of the DExD/H-box helicases RIG-I, MDA5, and LGP2 in antiviral innate immunity, J. Immunol. 175 (2005) 2851–2858.
[27] S. Takenaka, T. Kawayama, H. Imaoka, et al., The progression of comorbidity in IL-18 transgenic chronic obstructive pulmonary disease mice model, Biochem. Biophys. Res. Commun. 445 (2014) 597–601.
[28] M. Tominaga, M. Okamoto, T. Kawayama, et al., Overexpression of IL-38 protein in anticancer drug-induced lung injury and acute exacerbation of idiopathic pulmonary fibrosis, Respiratory investigation 55 (2017) 293–299.
[29] T. Nouno, M. Okamoto, K. Ohnishi, et al., Elevation of pulmonary CD163(+) and CD204(+) macrophages is associated with the clinical course of idiopathic pulmonary fibrosis patients, J. Thorac. Dis. 11 (2019) 4005–4017.
[30] T.S. Hageman, D.D. Weis, Reliable identification of significant differences in differential hydrogen exchange-mass spectrometry measurements using a hybrid significance testing approach, Anal. Chem. 91 (2019) 8008–8016.
[31] M. Sawada, T. Kawayama, H. Imaoka, et al., IL-18 induces airway hyperresponsiveness and pulmonary inflammation via CD4+ T cell and IL-13, PLoS One 8 (2013) e54623.
[32] T. Hoshino, R.T. Winkler-Pickett, A.T. Mason, et al., IL-13 production by NK cells: IL-13-producing NK and T cells are present in vivo in the absence of IFN-gamma, J. Immunol. 162 (1999) 51–59.
[33] D.C. Kang, R.V. Gopalkrishnan, Q. Wu, et al., mda-5: an interferon-inducible putative RNA helicase with double-stranded RNA-dependent ATPase activity and melanoma growth-suppressive properties, Proc. Natl. Acad. Sci. U. S. A. 99 (2002) 637–642.
[34] L. Alexopoulou, A.C. Holt, R. Medzhitov, et al., Recognition of double-stranded RNA and activation of NF-kappaB by Toll-like receptor 3, Nature 413 (2001) 732–738.
[35] S. Sato, K. Masui, N. Nishina, et al., Initial predictors of poor survival in myositis-associated interstitial lung disease: a multicentre cohort of 497 patients, Rheumatology 57 (2018) 1212–1221.
[36] M.L. Christensen, L.M. Pachman, R. Schneiderman, et al., Prevalence of Coxsackie B virus antibodies in patients with juvenile dermatomyositis, Arthritis Rheum. 29 (1986) 1365–1370.
[37] Y. Muro, K. Sugiura, K. Hoshino, et al., Epidemiologic study of clinically amyopathic dermatomyositis and anti-melanoma differentiation-associated gene 5 antibodies in central Japan, Arthritis Res. Ther. 13 (2011) R214.